Inverse estimation of Vc_{max}, leaf area index, and the Ball-Berry parameter from carbon and energy fluxes

Adam Wolf,[1,2] Kanat Akshalov,[3] Nicanor Saliendra,[4] Douglas A. Johnson,[5] and Emilio A. Laca[1]

Received 2 March 2005; revised 2 September 2005; accepted 21 September 2005; published 29 March 2006.

[1] Canopy fluxes of CO_2 and energy can be modeled with high fidelity using a small number of environmental variables and ecosystem parameters. Although these ecosystem parameters are critically important for modeling canopy fluxes, they typically are not measured with the same intensity as ecosystem fluxes. We developed an algorithm to estimate leaf area index (LAI), maximum carboxylation velocity (Vc_{max}), the Ball-Berry parameter (m), and substrate-dependent ecosystem respiration rate (β_A) by inverting a commonly used modeling paradigm of canopy CO_2 and energy fluxes. To test this algorithm, fluxes of sensible heat (H), latent heat (LE), and CO_2 (Fc) were measured with eddy covariance techniques in a pristine grassland-forb steppe site in northern Kazakhstan. We applied the algorithm to these data and identified ecosystem characteristics consistent with data across a time series of meteorological drivers from the Kazakhstan data. LAI was calculated by fitting the model to measured H + LE, Vc_{max} and β_A were solved simultaneously by fitting the model to measured CO_2 fluxes, and m was calculated by varying the partitioning of available energy between H and LE. Seasonal changes in LAI ranged from 2.0 to 2.4, Vc_{max} declined from 20 to 5 μmol CO_2 m^{-2} s^{-1}, respiration as a percentage of assimilation ranged from 0.5 to 0.75, and m varied from 17 to 24. Our results with the Kazakhstan data showed that LAI, Vc_{max}, ecosystem respiration, and m can be solved to accurately predict (R^2 = 80 to 95%) carbon and energy fluxes with nonsignificant bias at 20-min and daily timescales. The ecosystem characteristics calculated in our study were consistent with independent measurements of the seasonal dynamics of a shortgrass steppe in Kazakhstan and with values published in the literature. These characteristics were closely linked to mean daily fluxes of CO_2 but were not dependent on the environmental drivers for the periods they were measured. We conclude that process model inversion has potential for comparing CO_2 and energy fluxes among different ecosystems and years and for providing important ecosystem parameters for evaluating climatic influences on CO_2 and energy fluxes.

Citation: Wolf, A., K. Akshalov, N. Saliendra, D. A. Johnson, and E. A. Laca (2006), Inverse estimation of Vc_{max}, leaf area index, and the Ball-Berry parameter from carbon and energy fluxes, *J. Geophys. Res.*, *111*, D08S08, doi:10.1029/2005JD005927.

1. Introduction

[2] Evaluations of biogeochemistry and thermodynamics at an ecosystem scale with micrometeorological techniques are invaluable tools in understanding feedbacks between vegetation and the atmosphere [*Baldocchi et al.*, 2000; *Chapin et al.*, 2000; *Eugster et al.*, 2000; *McFadden et al.*, 2003; *McGuire et al.*, 2002]. However, the value of these measurements of high temporal resolution is limited to the extent that meaningful parameters of ecosystem function can be derived from these measurements for general interpretation [*Nichol et al.*, 2002; *Running et al.*, 1999]. The interpretation of measured fluxes of mass and energy are strictly dependent on the observed environmental drivers at the time of measurement, making generalizations and comparisons of ecosystem responses among sites and conditions problematic. Moreover, unless there is a basis for spatial extrapolation of measurements from specific tower sites to regional and global scales, it is difficult to use these data sets to evaluate important atmosphere-biosphere feedbacks at the regional and global scale [*Claussen et al.*, 2001; *Schulze*, 1995; *Sellers et al.*, 1996a, 1996b].

[1]Department of Plant Sciences, University of California, Davis, California, USA.
[2]Now at Department of Global Ecology, Carnegie Institution of Washington, Stanford, California, USA.
[3]Baraev Kazakh Research Institute for Grain Farming, Akmolinskaya oblast, Shortandy, Kazakhstan.
[4]U.S. Department of Agriculture Forest Service, Rhinelander, Wisconsin, USA.
[5]U.S. Department of Agriculture–Agricultural Research Service Forage and Range Research Laboratory, Utah State University, Logan, Utah, USA.

0148-0227/06/2005JD005927$09.00

[3] During the last decade, a wide variety of approaches have been used to model photosynthesis, respiration, energy balance, stomatal behavior, radiation transfer, and turbulent gas exchange on the basis of abundant data from flux tower experiments that measure these processes simultaneously, along with environmental drivers of mass and energy fluxes. As several research groups point out [*Lai et al.*, 2000; *Lloyd et al.*, 1995], most models have converged on approaches that use (1) a mechanistic biochemical model of leaf carbon fixation [*Farquhar et al.*, 1980] with variations provided by *Harley and Tenhunen* [1991], (2) an empirical model of stomatal control, especially the widely validated Ball-Berry equation [*Collatz et al.*, 1991], and (3) often a mechanistic physical treatment of radiation penetration and absorption at the canopy level where energy balance is considered [*de Pury and Farquhar*, 1997; *Norman*, 1993; *Sinclair et al.*, 1976; *Wang and Leuning*, 1998].

[4] These models require a small number of environmental drivers, namely incoming photosynthetically active radiation (PAR), air temperature (Tair), ambient CO_2 concentration (Ca), and relative humidity (rh) to simulate fluxes of CO_2 (Fc), water or latent heat (LE), sensible heat (H), net radiation (Rn) and ground heat flux (G) at any point in time, along with a small number of key canopy parameters and a respiration parameterization. The fundamental parameter in the *Farquhar et al.* [1980] model of plant biochemistry is the maximum carboxylation rate (Vc_{max}, μmol CO_2 per unit leaf area per second). Although net photosynthesis calculated by this model closely depends on the maximum rate of electron transport (J_{max}) and leaf maintenance respiration (Rd), these scale closely with Vc_{max} at a reference temperature [*Beerling and Quick*, 1995; *Reich et al.*, 1998; *Tanaka et al.*, 2002; *Wullschleger*, 1993]. Leaf area index (LAI) is also a key ecosystem descriptor because it determines the interception of radiation, which drives photosynthesis and energy exchange.

[5] The slope of the Ball-Berry equation has also emerged as a fundamental ecosystem descriptor. The Ball-Berry equation [*Collatz et al.*, 1991] calculates stomatal conductance (gs; mol m^{-2} s^{-1}) for water vapor in C3 plants as a function of net assimilation (A), leaf surface relative humidity (rh), leaf surface CO_2 concentration (Cs), minimum conductance (g_0), and a proportionality constant (**m**):

$$gs = m \cdot \frac{A \cdot rh}{Cs} + g_0 \tag{1}$$

[6] The value of **m** (also called the Ball-Berry parameter) appears to change from its base value under certain conditions, especially during drought [*Baldocchi*, 1997; *Lai et al.*, 2000; *Sala and Tenhunen*, 1996; *Tanaka et al.*, 2002; *Valentini et al.*, 1995]. Some authors, however, believe that **m** is a conserved property that changes little across biomes and environmental conditions [*Baldocchi and Meyers*, 1998; *Xu and Baldocchi*, 2003].

[7] The value of **m** is crucial because among the suite of biogeochemical and biogeophysical climate-biosphere feedbacks, accurate specification of stomatal conductance is fundamental in assessing future surface energy balance under various climatic change scenarios. Stomatal aperture is well known as a determinant of the partitioning of turbulent energy between sensible (H) and latent heat (LE) [*Monteith*, 1990]:

$$\frac{H}{LE} = \left(\frac{gb}{gs} + 1\right)\frac{dT}{VPD}\gamma \tag{2}$$

where gb is boundary layer conductance, dT and VPD are the temperature and vapor pressure difference between the ambient air and the canopy, respectively, and γ is the psychrometric constant.

[8] Ecosystem respiration (Reco) remains a major uncertainty in soil-plant-atmosphere modeling [*Hibbard et al.*, 2004]. Flux studies historically have relied on temperature functions to describe respiration, but a wide body of process studies demonstrate that ecosystem respiration is largely dependent on recent assimilation. Therefore, in the model we estimated Reco as a function of recent photosynthesis, but calculated the temperature dependency of nighttime Reco as an additional descriptor.

[9] Under experimentally controlled conditions, canopy parameters can be estimated from various data: Vc_{max} from A-Ci curves [*Harley and Baldocchi*, 1995; *Wullschleger*, 1993], **m** as the slope of the regression of A·rh/Cs on gs (see equation (1) and *Tanaka et al.* [2002] and *Xu and Baldocchi* [2003]), and LAI from various optical methods. However, collection of these data is labor-intensive, and measurements are obtained much less frequently than micrometeorological flux data. Because of these limitations, inversion of the complex process model to estimate parameters that best fit measured gas and energy fluxes holds considerable potential in estimating these key ecosystem characteristics. This would facilitate comparisons among ecosystems and years that would not be dependent on the particular weather conditions during the measurement period. In addition, this approach would allow estimation of landscape-level estimates of CO_2, H_2O, and energy fluxes.

[10] Some model inversion approaches have been used previously to extract ecosystem parameters from flux measurements [*Reichstein et al.*, 2003]. However, these previous approaches implicitly fix (or do not include) one or more of the three critical canopy parameters (LAI, Vc_{max}, and **m**) and do not constrain the solution of the unmeasured parameters using both CO_2 and energy fluxes. The first fundamental premise of our inversion approach is that Fc, LE, and H must all be used in constraining equations to estimate the three ecosystem parameters. Second, all these ecosystem parameters are highly interdependent [*Schulze et al.*, 1994] and must be solved simultaneously to satisfy all constraints. Finally, it is important to have as many equations as unknowns so that robust estimates can be obtained for the ecosystem parameters, because multicollinearity can dramatically increase the uncertainty of parameter estimates.

[11] In this paper we present a canopy flux model inversion approach that can be used to identify values of LAI, Vc_{max}, and **m** that are consistent with flux measurements and vary across the growing season. We

Table 1. List of Symbols Used in the Manuscript

Symbol	Units	Description
	Surface Fluxes	
G	W m^{-2}	ground heat flux
H	W m^{-2}	turbulent heat flux
LE	W m^{-2}	latent heat flux
LE_{eq}	W m^{-2}	Penman latent heat flux
Rn	W m^{-2}	net radiation
Fc	μmol CO_2 m^{-2} s^{-1}	net CO_2 flux
Reco	μmol CO_2 m^{-2} s^{-1}	ecosystem respiration
Rg	μmol CO_2 m^{-2} s^{-1}	growth respiration
β	…	Bowen ratio H/LE
λ	μmol CO_2/mmol H_2O	water use efficiency
	Meteorology	
Ca	μmol CO_2 mol^{-1} air	ambient CO_2 concentration
Cs	μmol CO_2 mol^{-1} air	leaf surface CO_2 concentration
Ci	μmol CO_2 mol^{-1} air	leaf internal CO_2 concentration
Tair	°C	air temperature
Tsoil	°C	soil temperature
PAR	μE m^{-2} s^{-1}	shortwave radiation 400–700 nm
NIR	W m^{-2}	shortwave radiation 700–2000 nm
VPD	kPa	vapor pressure deficit
s	kPa K^{-2}	slope of saturation vapor pressure curve
γ	mmol H_2O mol^{-1} air K^{-1}	psychrometric constant
ρ_{air}	mol m^{-3}	density of moist air
	Ecophysiology	
A	μmol CO_2 m^{-2} s^{-1}	leaf net assimilation rate per leaf area
Wj	μmol CO_2 m^{-2} s^{-1}	light limited carboxylation rate
Wc	μmol CO_2 m^{-2} s^{-1}	Rubisco limited carboxylation rate
Rd	μmol CO_2 m^{-2} s^{-1}	leaf maintenance respiration
g_s	μmol CO_2 m^{-2} s^{-1}	stomatal conductance
g_0	μmol CO_2 m^{-2} s^{-1}	minimum stomatal conductance
g_b	μmol CO_2 m^{-2} s^{-1}	aerodynamic conductance
Vc_{max}	μmol CO_2 m^{-2} s^{-1}	maximum carboxylation rate
Jmax	μmol e^- m^{-2} s^{-1}	maximum electron transport rate
LAI	m^2 leaf m^{-2} ground	leaf area index
m	. . .	Ball-Berry parameter
β_A	. . .	parameter relating Reco to assimilation
β_T	. . .	parameter relating Reco to temperature
kn	. . .	canopy nitrogen extinction coefficient

compare these ecosystem parameters with field measurements of grassland productivity. We then analyze the ecosystem parameters to determine if seasonal variation in **m** exists independent of changes in other ecosystem parameters.

2. Model Description

[12] In the basic form of the model, incoming solar radiation drives carbon assimilation in a two-layer canopy [*de Pury and Farquhar*, 1997; *Wang and Leuning*, 1998] according to the leaf-level biochemical model of *Farquhar et al.* [1980]. The stomatal conductance implied by carbon assimilation is solved according to a modified Ball-Berry equation [*Collatz et al.*, 1991] using the analytical method of *Baldocchi* [1994]. This stomatal conductance is used to solve the leaf's energy balance [*Paw U*, 1987; *Paw U and Gao*, 1988; *Su et al.*, 1996]. The meteorological variables needed to drive the model are PAR, air temperature, relative humidity, ambient [CO_2], wind speed, and time of day. The fundamental outputs of the model are fluxes of sensible heat (H), latent heat (LE) and CO_2 (Fc), which are key ecosystem processes measured using micrometeorological techniques. A table of symbols is provided in Table 1.

2.1. Micrometeorology

[13] Radiation intercepted by each of the two layers of the canopy is estimated using the equations of *de Pury and Farquhar* [1997], which accounts for direct and diffuse components of incoming radiation in the PAR and NIR bands, as well as reflection, scatter, and reabsorption of the intercepted radiation. In this radiation transfer model, the canopy's total leaf area is split into a "sun leaf," which intercepts both direct and diffuse light, and a "shade leaf," which intercepts only diffuse light. The partitioning of leaf area is contextual, as it depends on solar angle, canopy self-shading extinction coefficient, and LAI. Reflection and transmission coefficients of PAR and NIR are taken from *Goudriaan and van Laar* [1994] as reported for a typical grass, which are similar to the reported values of *Ripley and Saugier* [1978] for an *Agropyron*-dominated grassland in Saskatchewan, Canada.

[14] Boundary layer resistances (rb_{scalar}) for the exchange of mass and energy between the bulk atmosphere and the canopy surface are calculated using an aerodynamic resistance to momentum common to all scalars plus an excess

resistance for diffusion within the canopy specific to each scalar [*Kim and Verma*, 1990; *Monteith*, 1990]. We follow the paradigm of *Raupach* [1988] that resistances are expressed as inverse velocities (s/m) and conductances are expressed as flux densities (mol/m^2-s) according to the relation:

$$g_{scalar} = \rho_{air}/r_{scalar} \quad (3)$$

where ρ_{air} is the density of moist air.

2.2. Carbon Assimilation

[15] The carbon assimilation of the ecosystem is modeled using the *Farquhar et al.* [1980] paradigm of leaf photosynthesis [*Baldocchi and Meyers*, 1998; *Harley and Tenhunen*, 1991; *Leuning*, 1995], which postulates that gross assimilation is dependent on electron transport (Wj) and carboxylation (Wc) in series, and that the actual rate of assimilation is determined by the most limiting of these processes. Maximum carboxylation rate per leaf area under light-saturated conditions (Vc_{max}) is the fundamental determinant of assimilation in this model. The maximum rate of electron transport (Jmax) and leaf maintenance respiration (Rd) scale linearly with Vc_{max}. We used the values for biochemical scaling factors (2.3 for Jmax and 0.0046 for Rd at 25°C), kinetic parameters, and temperature functions reported by *Harley and Baldocchi* [1995]. The proportionality of 2.3 between Jmax and Vc_{max} is an intermediate value for grass species [*Wullschleger*, 1993].

[16] Solving the assimilation rate (A) depends on the internal CO_2 concentration of the leaf (Ci) ($Ci = Cs - A/gs_{CO2}$), which in turn requires an estimate of stomatal conductance of the leaf (gs_{CO2}) and leaf surface CO_2 concentration (Cs). The Ball-Berry equation [*Collatz et al.*, 1991] allows for stomatal conductance (gs) to be solved as a function of A, leaf surface relative humidity (rh), and Cs using the proportionality constant (**m**) and minimum conductance (g_0) (equation (1)), where $Cs = Ca - A/gb$ and $gb_{CO2} = \rho_{air}/rb_{CO2}$. Boundary layer relative humidity is calculated as the capacitance between supply of water vapor by stomata and loss of water vapor by aerodynamic conductance. Because A is dependent on Ci, Ci is dependent on gs, and gs is dependent on A, these equations need to be solved iteratively or simultaneously. *Baldocchi* [1994] proposed an analytical solution to the combined system of equations to solve for A, which in turn determines the solutions for all of the other variables simultaneously. Contrary to *Baldocchi*'s [1994] findings, we found that the correct root (one that gives a plausible value without an imaginary component) can vary under different environmental conditions, particularly at low rh. Therefore we included an algorithm to choose the correct root from a selection of *Baldocchi*'s [1994] roots, and the roots found by the program MATLAB [*MathWorks Inc.*, 1999].

2.3. Energy Balance

[17] The leaf energy balance model uses a two-sided representation of each leaf [*Monteith*, 1990; *Su et al.*, 1996]. Leaf temperature is calculated using a fourth-order polynomial for the saturation vapor pressure curve [*Paw U*, 1987], where all longwave radiation intake terms are doubled, as well as the H coefficient, to account for energy exchange on both sides of the leaf. A two-sided model allows for exchange of longwave radiation between the sunlit and shaded leaves, and is necessary to account for the different surfaces that exchange H and LE. H is exchanged from both sides of the leaf, but LE exchange only occurs to the extent that stomata are distributed on both sides of the leaf. A hypostomatous leaf only exchanges LE from one side of its surface, whereas an amphistomatous leaf exchanges LE from both surfaces. After stomatal conductance and leaf T are estimated in the carbon assimilation submodel, LE and H are determined for both the sun and shade leaves using standard resistance analog equations.

2.4. Respiration

[18] Respiration has three components: leaf maintenance respiration (Rd); plant growth respiration (Rg); and other ecosystem respiration (Reco). Rd is calculated at the same time as assimilation, and is assumed to scale linearly with Vc_{max} because it is closely linked to maintaining proteins used in photosynthesis [*Reich et al.*, 1998]. Rg is modeled as a stoichiometric product in the biochemical synthesis of proteins, carbohydrates, lipids, lignins and organic acids, which together compose stems, roots, leaves, seeds, and woody material of a plant [*Amthor*, 2000; *France and Thornley*, 1984; *Penning de Vries et al.*, 1974]. Plant samples collected at the time of the experiment were used to parameterize the partitioning of ecosystem growth among roots, stems, and leaves. The substrate supplied for growth is A (gross assimilation minus Rd). The specific growth rate of the ecosystem is set to 1, which is typical of young vegetation and implies that all photosynthate is immediately diverted to either structural growth or respired in the process [*France and Thornley*, 1984].

[19] Rd and Rg together account for a small proportion of observed respiration. Reco includes plant respiration expended in maintaining pressure gradients across cell membranes and repairing damaged nonphotosynthetic tissues, but is largely a combination of root respiration and heterotrophic soil respiration of labile root exudates [*Chapin and Ruess*, 2001], which can be a large proportion of net photosynthesis in rangelands [*Coyne et al.*, 1995]. A mechanistic understanding of ecosystem respiration is still elusive [*Hibbard et al.*, 2004], and currently respiration is modeled both as a function of (1) soil T and/or soil water content, which are thought to limit rates of autotrophic respiration [*Mielnick and Dugas*, 2000] or (2) as a function of photosynthetic rate, which represents a substrate limitation to respiration and is unaffected by T [*Craine et al.*, 1998; *Giardina and Ryan*, 2000]. Our model uses the substrate-limited approach to model ecosystem respiration, and calculates the respiration rate at any timestep as a proportion of the mean net assimilation of the previous 24 hours:

$$\alpha = \exp\left(\frac{-1}{(r*k)}\right) = 0.986 \quad (4)$$

$$A_i' = (A - Rd)_i - Rg_i \quad (5)$$

$$\bar{A}_i' = \bar{A}_{i-1}' * \alpha + A_i' * (1 - \alpha) \quad (6)$$

$$Reco_i = -\beta_A * \bar{A}_I' \quad (7)$$

where α is a digital filter coefficient, r is the sample rate (here seventy-two 20-min samples per day), k is the time constant (here 1 day), $\bar{A}_i'$ is the average net carbon assimilation for the previous 24 hours (μmol CO_2 m^{-2} land s^{-1}), and β_A is the rate of dark respiration as a fraction of net carbon assimilation rate. It follows that the minimum respiration rate occurs immediately prior to predawn (when the 24-hour mean assimilation is lowest), and the maximum respiration rate occurs at sunset, similar to the diurnal cycle for soil temperature. The coefficient is equivalent to the ratio of integrated respiration to integrated photosynthesis, and this is readily comparable to other indices of respiration to photosynthesis [*Gifford*, 2001].

[20] As a reference, nighttime respiration (μmol CO_2 m^{-2} land s^{-1}) was also fit to the temperature-dependent equation of *Mielnick and Dugas* [2000] with appropriate unit conversions:

$$\mathrm{Reco} = \beta_T * \exp(0.087 * \mathrm{Tsoil}) \tag{8}$$

where β_T is a parameter relating Reco to temperature.

2.5. Upscaling Leaves to Canopy

[21] The canopy was modeled as having two components, one receiving direct and diffuse light and the other receiving only diffuse light. The amount of leaf area assigned to each component was calculated at each instant, taking into account the sun's position and the extinction of light through the canopy. Just as LAI was partitioned into sunlit and shaded proportions varying throughout the day, canopy photosynthetic capacity was partitioned into sun and shade leaves using equations (15), (22) and (23) of *de Pury and Farquhar* [1997]. A putative Vc_{max} (maximum carboxylation rate per leaf area at the top of the canopy) was first integrated over the canopy using the N extinction coefficient (kn) [Canopy-Vc_{max} = LAI*Vc_{max}*$(1-e^{-kn})$/kn], and then assigned to each component, taking into account the partition of LAI between the two components as a function of the sun's position. Values of kn for grasses reported in the literature vary widely, e.g., from 0.713 (wheat [*de Pury and Farquhar*, 1997]) to 0.136 [*Leuning*, 2000]; we chose kn = 0.5. Canopy-Vc_{max} scales linearly with either Vc_{max} (subject to LAI held constant) or LAI (subject to Vc_{max} held constant), and is approximately the same as Vc_{max}*LAI.

[22] Total canopy fluxes of H, LE and Fc were calculated by adding the specific fluxes of H, LE and A of the sun and shade leaves multiplied by their leaf area [*Norman*, 1993], plus Rg and Reco. During wet periods, LE was modeled as the equilibrium evaporation from a wet surface [LE_{eq} = (Rn−G)*s/(s + γ)] [*Monteith*, 1990], where Rn is net incoming energy, G is ground heat flux and storage, s is the slope of the saturation vapor pressure-temperature curve, and γ is the psychrometric constant.

2.6. Fitting the Model to Measured Fluxes

[23] The modeled fluxes were fit to the measured fluxes of H, LE and Fc using a least squares procedure to find the set of ecosystem parameters that are most consistent with the data, given a time series of meteorological drivers. The complete set of fitted ecosystem parameters included leaf area index (LAI), maximum leaf carboxylation rate (Vc_{max}), stomatal sensitivity (**m**), and β_A. Given a time series of Fc alone, it would not be possible to robustly determine both LAI and Vc_{max}, because these both have strong positive effects on Fc. However, we hypothesize that the total outgoing energy (H + LE) is only weakly determined by Vc_{max} (through its effect on A and thereby on gs). Thus, given a reasonable estimate of Vc_{max}, LAI can be solved using the energy balance alone because absorbed radiation (and canopy albedo) is strongly dependent on leaf area [*Sellers et al.*, 1992]. The following system of equations was iterated until convergence:

[24] 1. LAI (given an estimate of Vc_{max}, β_A and **m**) was solved by varying LAI to fit the total energy balance H + LE:

$$\min \sum \left((H+LE)_{model} - (H+LE)_{measured} \right)^2 \tag{9}$$

[25] 2. Vc_{max} and β_A (given LAI and estimate of **m**) were solved simultaneously by fitting the modeled net ecosystem exchange (Fc) to the measured Fc, using a nonlinear search algorithm in Matlab's Optimization Toolbox [*MathWorks Inc.*, 1999]:

$$\min \sum (Fc_{model} - Fc_{measured})^2 \tag{10}$$

[26] 3. **m** (given LAI, Vc_{max} and β_A) was solved by varying **m** to fit both LE and H:

$$\min \left(\sum (H_{model} - H_{measured})^2 + \sum (LE_{model} - LE_{measured})^2 \right) \tag{11}$$

[27] 4. LAI, Vc_{max}, and β were solved using the solved **m**.

[28] Uncertainty of the parameters was estimated by perturbing each parameter in turn and calculating their standard deviations using the procedure adapted from *Neter et al.* [1996], where i = 1,. . ., n observations, j = 1,. . ., p parameters, and g* = $\{g_1, g_2, g_3, \ldots g_p\}$ is the solution set of p parameters that compose the ecosystem state:

[29] 1. First, we calculated predicted values and errors:

$$\hat{Y}_i = f(X_i, g^*) \tag{12}$$

$$e_i = Y_i - \hat{Y}_i \tag{13}$$

$$\mathrm{MSE} = e'e/\mathrm{dfe} \text{ where } \mathrm{dfe} = n - p \tag{14}$$

where Y is the flux measurement used to solve the parameter (e.g., H + LE for LAI, Fc for Vc_{max} and β_A, H and LE for **m**).

[30] 2. Second, we calculated the n by p matrix of partial derivatives of each predicted value with respect to each parameter using a small perturbation dg_j, evaluated at g*:

$$D[i,j] = df(X_i, g^*)/dg_j | g = g^* \tag{15}$$

[31] 3. Finally, we calculated a variance-covariance matrix, where the square roots of the diagonal elements were the standard deviations of the parameters:

$$S^2\{g\} = \mathrm{MSE}^* (D'D)^{-1} \tag{16}$$

[32] Data that are noisy or poorly fit by the model will have a large MSE, which leads to larger confidence inter-

vals around the solved parameter. We used a mechanistic model that integrates most of what is accepted about herbaceous canopy photosynthesis and energy flows to partition the variance in of our data into explained and unexplained variation. Interpretations for filling data gaps, and for management and decision making are based on the explained variation and patterns. Residuals were interpreted to determine when the model fails and for future research purposes.

3. Experimental Data

3.1. Site Description

[33] The study site is located 40 km north of Astana, Kazakhstan and 20 km south of the Baraev Kazakh Research Institute for Grain Farming (NIIZern) in Shortandy. The latitude-longitude of the site is 51°34′33″N, 71°16′05″E, and elevation is 428 m above sea level. The experimental area is a 200-ha pristine grassland-forb steppe within NIIZern that was excluded from wheat cultivation, and is considered a true steppe, representative of rangelands extending from northern Crimean lowlands through the southern Russian Plain to the steppes of northern Kazakhstan. The vegetation at the site is dominated by C3 grasses *Stipa capillata, Stipa lessingiana*, and *Agropyron cristatum*, and other species including *Kochia prostrata*, *Medicago falcata*, *Festuca valesiaca*, *Artemisia marshalliana*, and *Artemisia glauca*. Soils are classified as Pachic Huplustolls. Long-term average annual air temperature (1961–2001) at NIIZern is 1.1°C, and total annual precipitation is 340 mm. Climate is characterized by a summer maximum of precipitation with generally favorable growth conditions during the growing season. Precipitation varies widely among years with up to 50% of the years exhibiting drought in June and sometimes in July.

[34] Topography at the site is flat with homogeneous vegetation, which is well suited for micrometeorological flux measurements. The fetches for upwind directions were 250 m from the north, 610 m from the east, 2,250 m from south, and 360 m from the west. The predominant wind comes from the southeast. A field road separated the site from a wheat field on the west, and another field road separated the site from a fallow field on the north.

[35] We used data from five periods during the growing season in 2001 when two flux towers were colocated on the pristine steppe site described above. The measurements were obtained from the spring period when fields became traversable (Julian day 152) to the late-season period prior to snowfall (day 256).

3.2. Eddy Covariance Methods

[36] Fluxes of CO_2, water, and heat were measured using an eddy covariance system (EC) based on a fast response open-path infrared gas analyzer (IRGA, Model LI-7500, Licor, Inc. Lincoln, Nebraska) coupled with a three-dimensional sonic anemometer (Model CSAT-3, Campbell Scientific, Logan, Utah). The sensors were placed at 1.8 m, and the canopy height was about 0.30 m. Digital signals from these instruments were recorded at 10 Hz using a Campbell Scientific CR5000 datalogger. All raw data were archived for later postprocessing. Additional aerial instrumentation included two net radiometers (Model Q*7.1, REBS, Seattle, Washington), a combined temperature/humidity sensor (Model HMP45C, Campbell Scientific), and a PAR sensor (Model LI190SB, Campbell Scientific). Ground heat flux was measured at an 8-cm depth by six heat flux plates (two Model HFT3, REBS and four Model HFP01SC, Hukseflux Thermal Sensors, Netherlands). Heat storage in the soil was calculated from temperature using three averaging soil temperature probes (Model TCAV, Campbell Scientific) installed above the soil heat flux plates (at 2 and 6 cm depth) and volumetric soil water content measured by three water content reflectometers (Model CS615, Campbell Scientific). Reflectometer output was calibrated to volumetric soil moisture content from soil samples periodically obtained throughout the study.

[37] Gas concentration, temperature, and wind speed data were processed in several steps, each of which was found to have a significant effect on the resultant flux. Raw data were first separated into 20-min intervals and adjusted for time lags in the H_2O and CO_2 channels by maximizing the cross correlation between the gas measures and vertical wind speed. Fluxes for each 20-min interval were calculated by (1) computing the covariance between each scalar (H_2O, CO_2, and T) with vertical wind speed, (2) rotating the fluxes to a natural coordinate system [*Tanner and Thurtell*, 1969], (3) adjusting for air density artifacts [*Webb et al.*, 1980], (4) iterating the WPL correction to estimate true temperature from sonic temperature, and (5) correcting for sensor frequency-response losses [*Massman*, 2000]. No fluxes were discarded on the basis of low turbulence. Although the landscape is a flat shortgrass steppe and the measurements were taken at a high frequency, we found that the frequency response corrections had a substantial effect, similar to those reported by *Eugster et al.* [1997]. CO_2 fluxes are reported using the meteorological convention that canopy uptake is negative and respiration is positive.

4. Results

4.1. Energy Balance Closure

[38] Measured energy balances were nearly closed during the study period, showing an overall closure of 90%. The regression of measured H + LE on measured Rn-G had an R^2 of 92.7% with a slope of 0.905 (se = 0.007) and intercept of −3.30 (se = 1.23) (Figure 1).

4.2. Model Performance

[39] The model closely tracked 20-min values of measured energy fluxes in most cases (Table 2). The model predicted total energy (TE = H + LE) with the greatest accuracy (R^2 = 90–95%) in all measurement periods with a slope and intercept not significantly different from 1.0 and 0.0, respectively.

[40] Available energy estimated by the model closely matched the Rn-G measured at the site (Figure 1). Modeled energy fluxes (H_{mod} + LE_{mod}) matched measured H + LE. H and LE were also modeled with high fidelity, although modeled LE were on average 11% higher than measured LE values (Table 3). Incoming energy was partitioned accurately between H and LE with no observed bias (Figure 2).

[41] Fluxes of CO_2 were also estimated reasonably well with the model having a slope near 1.0 and an intercept

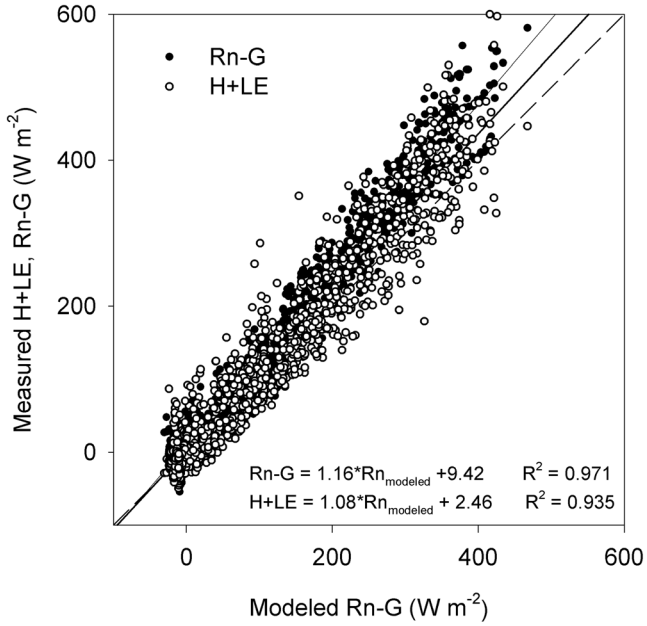

Figure 1. Modeled available energy versus measured Rn-G-S (solid circles) and H + LE (open circles).

near 0.0. Both the substrate-dependent model and the temperature-dependent model generated similar nighttime CO_2 flux estimates (Figure 3), although there is substantial unexplained variation in measured nighttime respiration, probably a consequence of sporadic turbulence during periods of high stability of the nocturnal boundary layer [*Moncrieff et al.*, 1996].

4.3. Seasonal Changes in Modeled LAI, Vc_{max}, β_A and m

[42] This approach yielded precise estimates of LAI, Vc_{max}, m and β_A (Table 3) with average coefficients of variation over periods being 0.009, 0.054, 0.034, and 0.079. Modeled LAI changed little during the course of the flux measurements, ranging from 2.0 to 2.5 (Figure 4). LAI initially dropped, which corresponded to the flowering and seeding period of the dominant grass. On the basis of measured aboveground biomass (Figure 5), this corresponded to an initial specific leaf area (SLA, area/mass) of 0.012 $m^2\ g^{-1}$, a low of 0.008 $m^2\ g^{-1}$ during flowering, and a high of 0.0156 $m^2\ g^{-1}$. These SLA values are typical for leaves under low-light or low-N conditions.

[43] Vc_{max} decreased dramatically during the growing season (Figure 6) from a high of 20.0 to a low of 5.4 μmol CO_2 m^{-2} s^{-1} on a leaf area basis and from 36.8 to 10.5 μmol CO_2 m^{-2} s^{-1} integrated over the canopy. This decrease corresponded to a 75% decrease in measured mean daily photosynthesis.

[44] The Ball-Berry parameter varied during the growing season from a low of 15 (favoring H over LE) to a high of 24 (favoring LE over H) (Figure 7a). This seasonal pattern of variation echoes observed changes of mean daily energy partitioning. Positive deviations from the global trend of **m** correspond to negative deviations of Bowen ratio (β) (Figure 7d), and β shows the expected inverse relationship with soil water content (Figure 7b). Likewise, the ratio of

Table 2. Parameters for Instantaneous (20 min) Modeled Versus Measured Fluxes[a]

	n	A	B	R^2	RMSE
Period 1, days 156–158					
Fc	464	1.14 (0.026)	−0.42 (0.12)	0.810	2.12 μmol CO_2 m^{-2} s^{-1}
LE	465	0.81 (0.021)	26.50 (2.43)	0.755	41.0 W m^{-2}
H	470	0.98 (0.021)	−11.91 (1.75)	0.820	33.8 W m^{-2}
TE	470	0.96 (0.011)	4.81 (2.18)	0.936	38.6 W m^{-2}
Period 2, days 181–184					
Fc	242	1.02 (0.029)	−0.09 (0.10)	0.838	1.35
LE	256	0.78 (0.027)	8.32 (2.65)	0.764	30.6
H	256	0.95 (0.023)	6.26 (1.76)	0.861	24.5
TE	256	0.90 (0.018)	8.34 (3.06)	0.905	38.3
Period 3, days 207–211					
Fc	360	1.01 (0.021)	−0.06 (0.07)	0.866	1.31
LE	360	1.09 (0.014)	−8.80 (1.60)	0.939	21.2
H	360	0.92 (0.013)	0.31 (1.07)	0.931	17.4
TE	360	1.04 (0.012)	−8.85 (2.19)	0.955	31.7
Period 4, days 231–234					
Fc	288	0.95 (0.037)	−0.00 (0.10)	0.701	1.59
LE	288	0.82 (0.024)	8.91 (2.02)	0.795	26.5
H	288	0.99 (0.021)	−2.63 (2.02)	0.880	30.4
TE	288	0.92 (0.014)	4.09 (2.45)	0.936	34.5
Period 5, days 256–257					
Fc	111	0.88 (0.101)	0.13 (0.12)	0.41	1.23
LE	121	0.82 (0.052)	0.93 (1.82)	0.675	15.5
H	121	1.03 (0.034)	3.17 (2.12)	0.885	20.4
TE	121	0.95 (0.025)	3.91 (1.76)	0.820	33.8
All periods					
Fc	1465	1.05 (0.013)	−0.13 (0.05)	0.811	1.67
LE	1490	0.89 (0.011)	9.37 (1.13)	0.806	33.2
H	1495	0.96 (0.010)	−2.89 (0.83)	0.859	28.1
TE	1495	0.98 (0.006)	2.82 (1.14)	0.934	35.7

[a]The regression model is measured flux = a * modeled flux + b.

Table 3. Calculated Values for Ecosystem Parameters (With Standard Deviations in Parentheses), Mean Daily Fluxes, and Mean Environmental Variables for Each Measurement Period[a]

Period	LAI, m^2 m^{-2}	Vc_{max}, μmol CO_2 m^{-2} s^{-1}	Canopy-Vc_{max}, μmol CO_2 m^{-2} s^{-1}	**m**	β_A	β_T	
1	2.34 (0.02)	19.92 (0.76)	36.68	17.0 (0.40)	0.52 (0.03)	0.81 (0.04)	
2	2.04 (0.02)	17.53 (0.63)	28.14	15.8 (0.36)	0.65 (0.03)	0.63 (0.04)	
3	2.22 (0.01)	15.37 (0.42)	26.85	18.4 (0.15)	0.67 (0.02)	0.65 (0.03)	
4	2.35 (0.02)	9.28 (0.43)	17.16	15.4 (0.47)	0.75 (0.04)	0.57 (0.04)	
5	2.49 (0.04)	4.51 (0.56)	8.84	23.8 (2.02)	0.53 (0.11)	0.27 (0.09)	
Period	Daytime Fc, μmol CO_2 m^{-2} day^{-1}	Nighttime Fc, μmol CO_2 m^{-2} day^{-1}	LE, KW m^{-2}	PAR, uE/day	Ta, °C	RH, %	vsmc, %
1	251.8	59.59	6.39	32086	16.2	61.0	0.25
2	184.3	65.93	4.77	30902	16.0	66.6	0.20
3	151.4	62.57	5.35	39433	19.3	48.0	0.26
4	91.3	58.96	3.58	27035	17.7	62.1	0.12
5	62.9	26.59	0.91	14431	8.4	68.5	0.14

[a]PAR is incoming photosynthetically active radiation, Ta is air temperature, RH is relative humidity, and vsmc is volumetric soil moisture content.

CO_2 uptake to H_2O loss (λ) varies substantially over the season, and is consistent with modeled variations in **m**, where higher **m** is linked to lower λ (Figure 7c). Strong inferences about the variation in **m** is clouded by the substantial day-to-day variation in both β and λ; values of **m** from 15 to 20 would fit relatively well across the season.

[45] Ecosystem respiration parameters as a proportion of photosynthesis showed a marked increase during the growing season, but decreased as a function of temperature during the growing season (Figure 8a). These corresponded to an increase in root mass, and proportion of roots as biomass during the same period (Figure 5). However, measured mean daily respiration rate was relatively constant during the growing season, except during the final measurement period (Figure 8a).

4.4. Diurnal Patterns of CO_2 and Energy Fluxes

4.4.1. Similarities Between Measurements and Model Results

[46] The time series of LE (Figure 9), H (Figure 10) and Fc (Figure 11) showed close agreement between the measured fluxes and radiative forcing, which is the key daytime driving variable in the model. Measured midday spikes in LE, H and Fc, which were caused by cloud interception of PAR, were closely tracked at the 20-min scale by the model on many days (e.g., day 181, day 234). Time series analysis in the frequency domain ("stimulus-response" [*Shumway and Stoffer*, 2000]) showed that measured H and LE were driven by the meteorological conditions at the time of measurement with no lagged drivers. However, using the same analysis, Fc was significantly driven by present conditions as well as conditions in the 20-min period preceding the measurement, indicating a biophysical lag that was not included in the model, or a timestep that may be too short for modeling CO_2 fluxes.

4.4.2. Discrepancies

[47] On several nonrainy days, midday LE was systematically underestimated (day 155, day 184, day 210, day 211) or overestimated (day 152, day 233) (Figure 9); H was correspondingly overestimated and underestimated (Figure 10). Overestimates of LE (day 152) followed a prolonged dry period (data not shown), and some underestimates of LE followed rainfall events (day 155, day 184). The model also highlighted several instances of possible measurement error, when environmental conditions could not plausibly lead to the observed fluxes. Some of these instances were traced to rainfall, which is an obvious source of sensor error (e.g., LE in the evening on day 153, Figure 9; H during midday on day 182, Figure 10; Fc in the morning of day 256, Figure 11). However, there were also periods where the model substantially departed from measured flux values for major portions of nonrainy days, especially for Fc (e.g., day 232, day 233, Figure 11).

[48] Nighttime Fc measurements occasionally matched modeled Fc values, but there are clearly more sources of variation in respiration than recent photosynthesis. On some days poor agreement appeared to be related to measurement uncertainty related to wet sensors or intermittent turbulence (after day 183, day 210, Figure 11), but on several days with apparently smooth Fc data, modeled Fc values did not agree with actual data. Neither measured soil water content nor temperature accounted for these variations in nighttime Fc

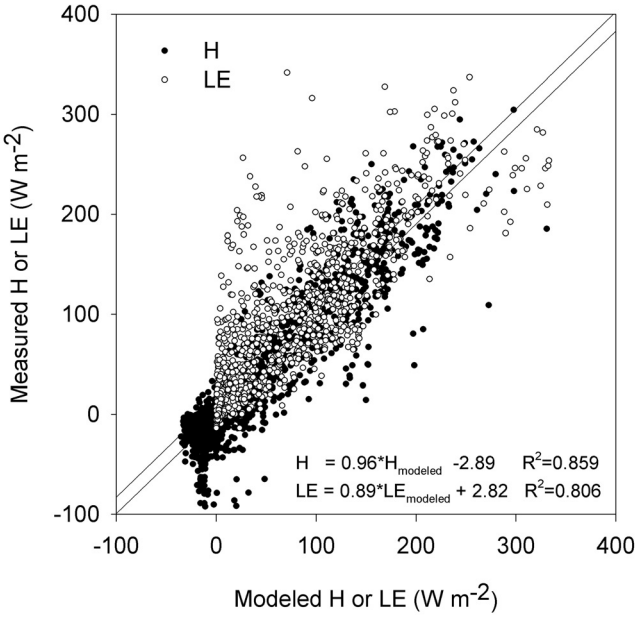

Figure 2. Modeled H (solid circles) and LE (open circles) components of energy balance versus eddy covariance measurements.

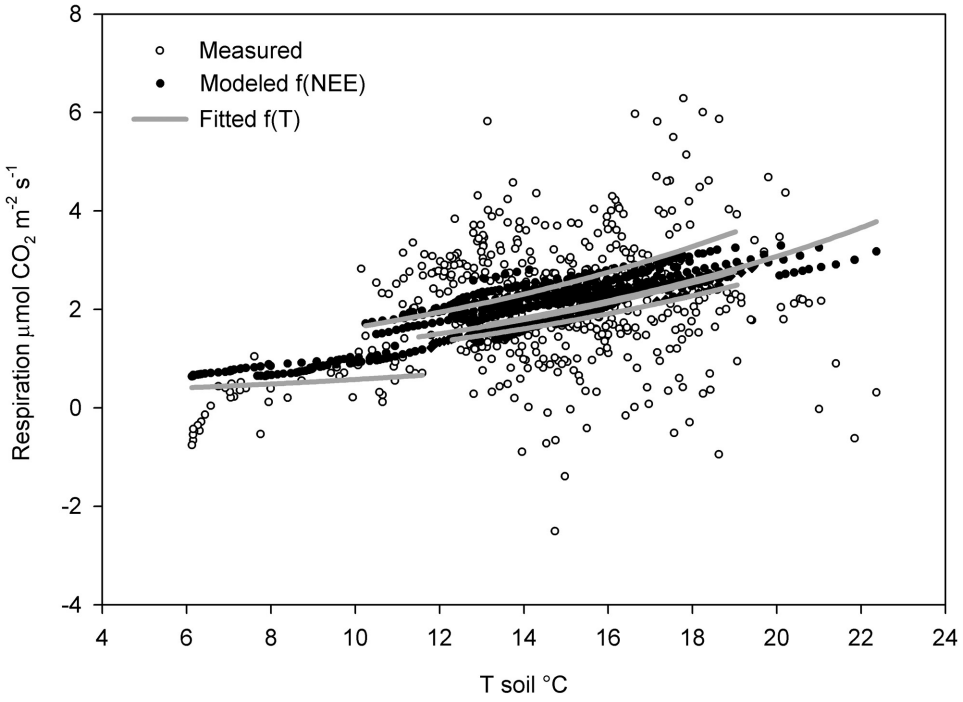

Figure 3. Measurements of nighttime respiration at 20-min resolution (open circles), versus respiration estimated using a substrate-dependent model (solid circles) and a temperature-dependent model (shaded lines).

values because both varied more slowly than the CO_2 fluxes.

4.4.3. Rainy Periods

[49] During rainy periods, predicted values of LE differed substantially from actual LE. Although some of these differences were due to wet sensors, measured LE during wet periods (days 154–157, days 182–183, days 231–232, day 257, Figure 9) were very similar to equilibrium evaporation expected from a wet surface. This suggests that the IRGA and sonic anemometer sensors may sometimes provide plausible estimates of water vapor and CO_2 fluxes in the rain.

[50] The greatest departures of predicted compared to actual H fluxes occurred at night during rainy periods (e.g., days 153–156, Figure 7). Negative fluxes can occur in a canopy that is cooler than the surrounding air, leading to sensible heat flux into the surface. The model predicted downward LE flux during these periods (i.e., condensation). This lack of agreement between modeled values and actual measurements indicates possible physical cooling from intercepted rain rather than condensation.

4.5. Daily Integrals

[51] It is important that daily flux estimates are accurate because a key benefit of the model will be to provide flux estimates from 20-min timescales to multiday timescales using driving data at various temporal scales. Besides accurately predicting fluxes at a 20-min timescale, the model was able to predict integrated daily fluxes (Figure 12). None of the slopes between the modeled and measured values were significantly different from 1.0 ($P > 0.05$), and none of the intercepts were significantly different from 0.0. Similar to the regressions using instantaneous fluxes, the model best predicted total turbulent energy fluxes (H + LE). Individual turbulent energy fluxes showed considerable variability, particularly for H.

[52] The estimation of Fc at a daily scale was relatively accurate (R^2 = 72.6%) and unbiased (slope = 1.25); however, these results obscured the poor prediction of nighttime CO_2 flux. The nighttime flux on a daily scale was not

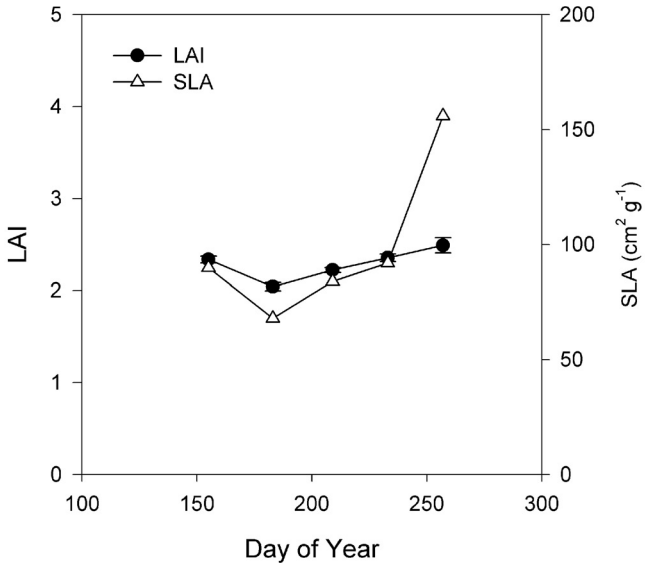

Figure 4. Seasonal course of modeled LAI. Specific leaf area (SLA) was inferred from combining model estimates with field measurements of aboveground green biomass.

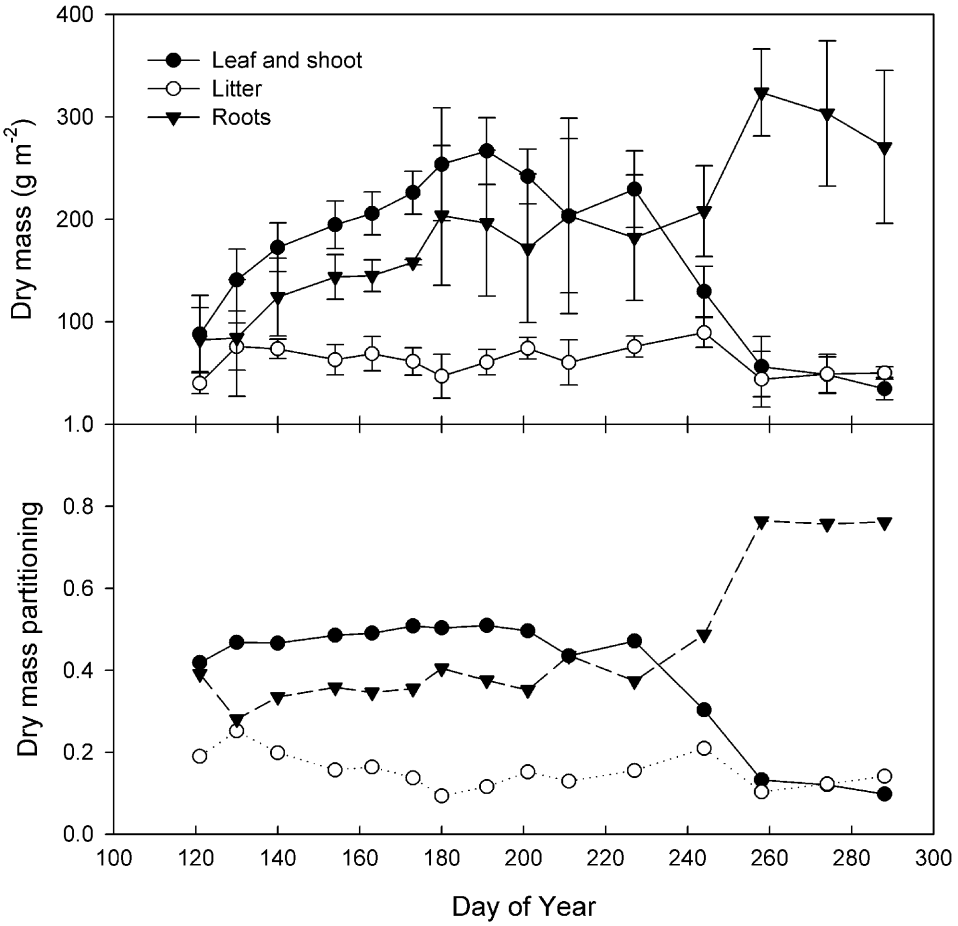

Figure 5. Measured seasonal changes in aboveground and belowground biomass from field samples.

related to nighttime air temperature, soil temperature, soil water content, or friction velocity.

5. Discussion

[53] The number of long-term, continuous measurements of CO_2 and energy fluxes using micrometeorological techniques has grown dramatically in the last decade [*Baldocchi et al.*, 2001]. The key advantage of such a network of field measurements is the intercomparability of results among widely varying ecosystems and climatic conditions. Global comparisons of leaf level attributes from disparate ecosystems have shown a remarkable degree of convergence of attributes, which determine the tradeoff of carbon acquisition and water loss [*Reich et al.*, 1997; *Schulze et al.*, 1994]. At the ecosystem scale, aggregate comparisons of flux tower observations showed that differing biomes have broadly similar patterns of water use efficiency and photosynthesis:respiration partitioning at an annual timescale [*Law et al.*, 2002]. Because optimization apparently leads to convergence for some ecosystem attributes, process models with simplified representations of leaf biochemistry, energy exchange, stomatal behavior, and canopy light interception have been able to reproduce ecosystem flux observations in a wide number of ecosystems with high fidelity using a small number of ecosystem-specific parameters, namely leaf area, leaf photosynthetic capacity [*Baldocchi and Meyers*, 1998], stomatal sensitivity (expressed as variation in the

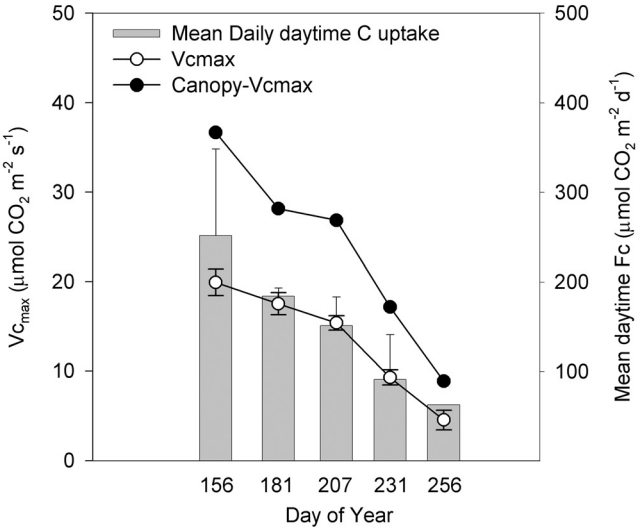

Figure 6. Seasonal course of modeled changes in maximum carboxylation velocity (Vc_{max}) per leaf area (open circles) and per canopy area (solid circles). Vertical bars show mean daytime carbon uptake by the ecosystem measured by eddy covariance for each measurement period starting at the day on the *y* axis. Note that positive values denote uptake of CO_2.

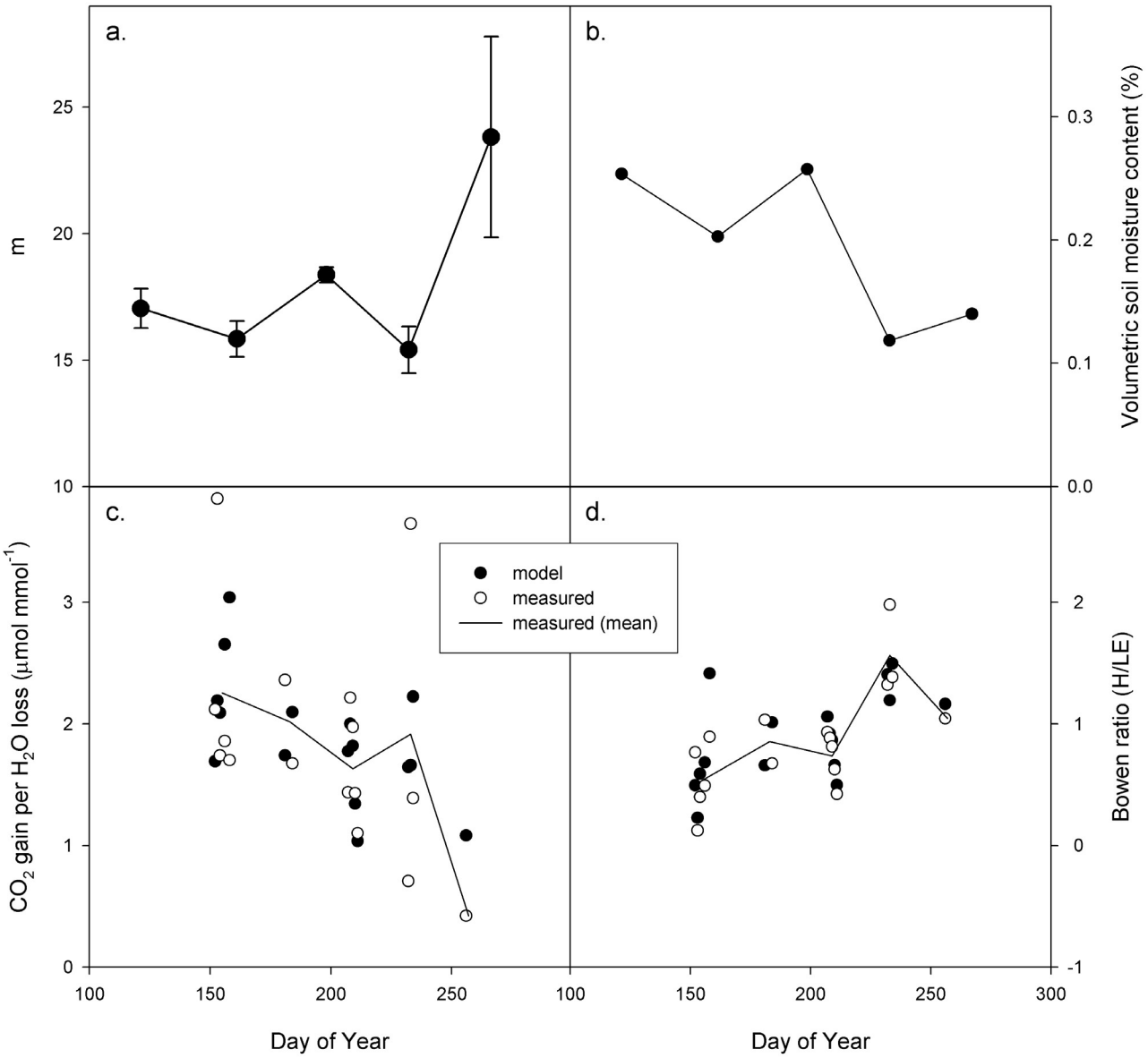

Figure 7. Seasonal variation in indicators of stomatal conductance: (a) modeled changes in the Ball-Berry parameter (**m**), (b) seasonal change in volumetric soil moisture content, (c) seasonal variation in unit CO_2 gain per unit evaporation, and (d) seasonal variation in Bowen ratio. Figures 7c and 7d show mean daytime values excluding periods with precipitation. Open circles are calculated from measured fluxes; solid circles are calculated from modeled fluxes. Line shows mean of measured values for each period.

Ball-Berry parameter **m**) [*Baldocchi*, 1997; *Lai et al.*, 2000], and ecosystem respiration rate.

[54] Values of LAI and Vc_{max} are fixed parameters at the timescale of a few days, when canopy N and C balance are relatively constant. Seasonal changes in the Ball-Berry parameter have been used to explain changes in Fc and LE that are inconsistent with estimates of LAI and Vc_{max}, suggesting that it too is dynamically controlled [*Baldocchi*, 1997; *Sala and Tenhunen*, 1996; *Lai et al.*, 2000]. In addition, ecosystem nonleaf respiration, which is largely dependent on root respiration and root exudation of photosynthate [*Craine et al.*, 1998], is a fixed parameter only to the extent that plant photosynthate supply to roots is constant. During the growing season, these descriptors are more accurately termed state variables, since collectively they determine the exchange of CO_2, water and heat, and therefore describe the state of the ecosystem at any point in time.

[55] Environmental conditions, of course, vary across the world, and ecosystem optimization results in plant phenologies that depend on the local environment (disturbance and aerial, hydrological, edaphic conditions). Reasonable predictions of carbon and energy exchange are possible if the ecosystem parameters are known. Currently, measurements of spatial and temporal variation in fluxes far exceeds measurements of these above mentioned state variables.

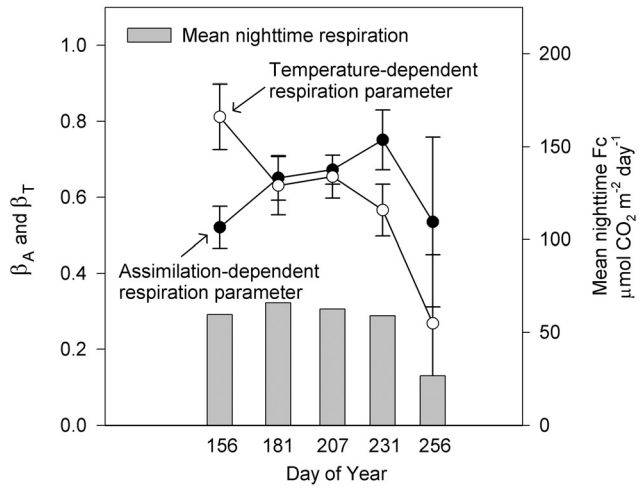

Figure 8. Seasonal course of modeled changes in parameters for assimilation-dependent (solid circles) and temperature-dependent (open circles) rates of nighttime ecosystem respiration. Vertical bars show mean nighttime carbon loss by the ecosystem measured by eddy covariance for each measurement period starting at the day on the *y* axis.

This may be because direct measurement of these parameters takes considerable additional effort beyond that required for flux measurements and because not all flux measurement projects are directly linked to a flux modeling effort. Knowing the values of these parameters and their seasonal patterns will assist in the spatial extrapolation of flux data.

[56] Differences in methodology for determining these ecosystem attributes make comparisons among sites difficult. For example, *Sala and Tenhunen* [1996] used an inverse approach to solve for **m** across the growing season. They found that **m** changed dramatically during the season and was strongly associated with predawn xylem water potential. They concluded that **m** was the only key phenotypical parameter that determined Fc and LE. However, they based their conclusion on an inversion approach that depended on single values of LAI and Vc_{max} for the entire season, based on previous results that showed that Vc_{max} was not affected by drought. LAI and Vc_{max} (or leaf N) do change during the growing season, and this likely allows plants to sychronize their photosynthetic capacity with both nutrient and water availability.

[57] The methods of *Sala and Tenhunen* [1996] differed from that of *Xu and Baldocchi* [2003] who directly measured leaf photosynthesis and other environmental variables in the field to estimate Vc_{max} and the slope of the Ball-Berry equation. *Xu and Baldocchi* [2003] concluded that **m** was constant through the season and not influenced by drought. However, deviations from the Arh/cs – gs regression in *Xu and Baldocchi*'s [2003] study were not evaluated in relation to soil, xylem, or leaf water potential to directly address the possibility that **m** does vary in response to environmental conditions.

[58] *Lai et al.* [2000] directly measured LAI and **m** throughout the season and also measured Vc_{max} twice during a 2-year study. They used Fc, LE and H to constrain the parameters used in model simulations, and found that soil water content and **m** were associated, which they used to develop a correction factor for **m** when soil water content dropped below a threshold value. However, because Vc_{max}

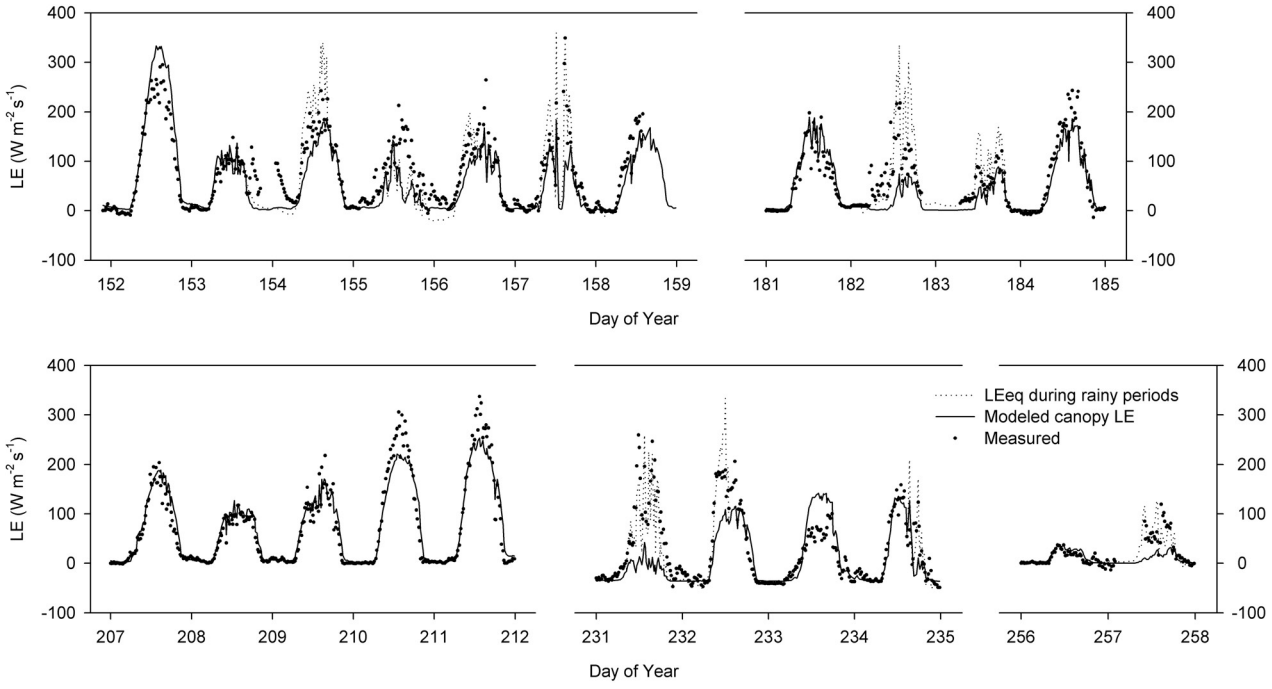

Figure 9. Daily course of latent heat flux (LE) for 22 days during the growing season. Dots are LE measurements, the solid line is the LE predicted using a combined energy balance-carbon assimilation model, and the dotted line is equilibrium LE (dependent only on available energy) during wet periods.

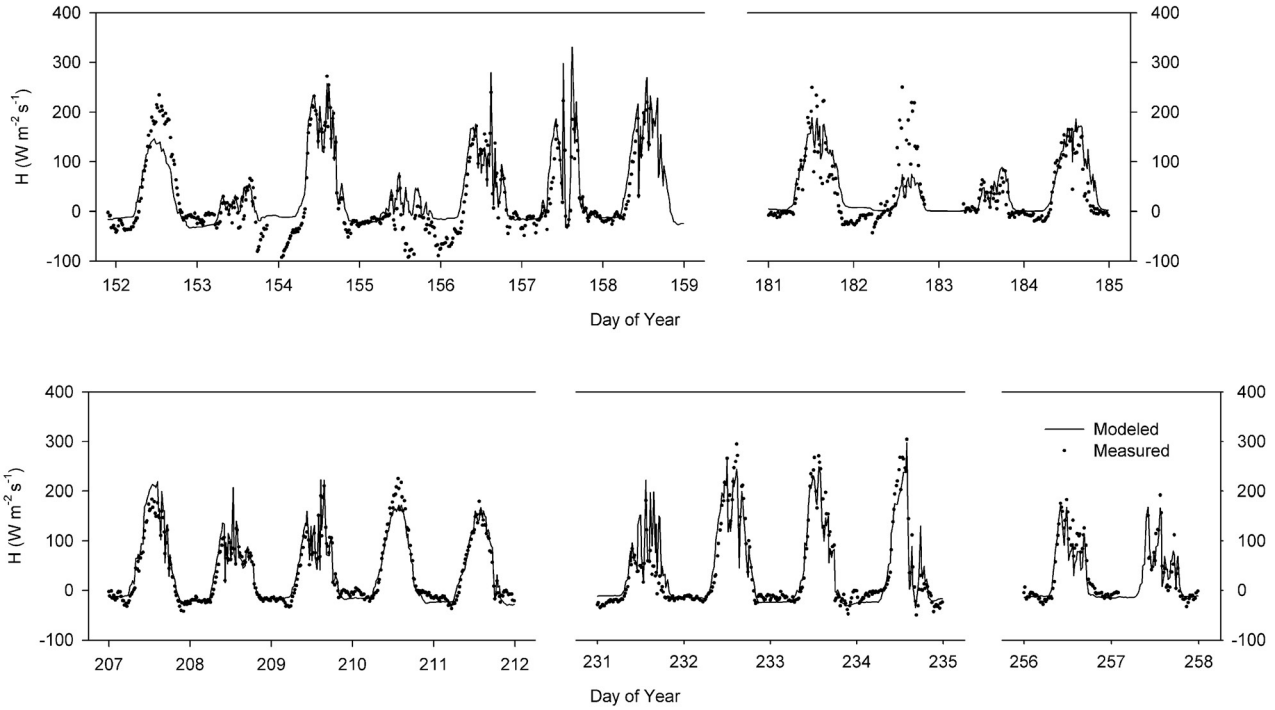

Figure 10. Daily course of sensible heat flux (H) for 22 days during the growing season. Dots are H measurements, and the solid line is predicted H using a combined energy balance-carbon assimilation model.

was assumed constant throughout the season (subject to a temperature adjustment), unmeasured seasonal changes in Vc_{max} may be partly responsible for observed variations in apparent **m**.

[59] *Reichstein et al.* [2003] used an elaborate model inversion approach in which Vc_{max}-**m** and LAI-**m** were independently fitted to Fc and LE relationships. Using a single response variable to fit two parameters, they averaged

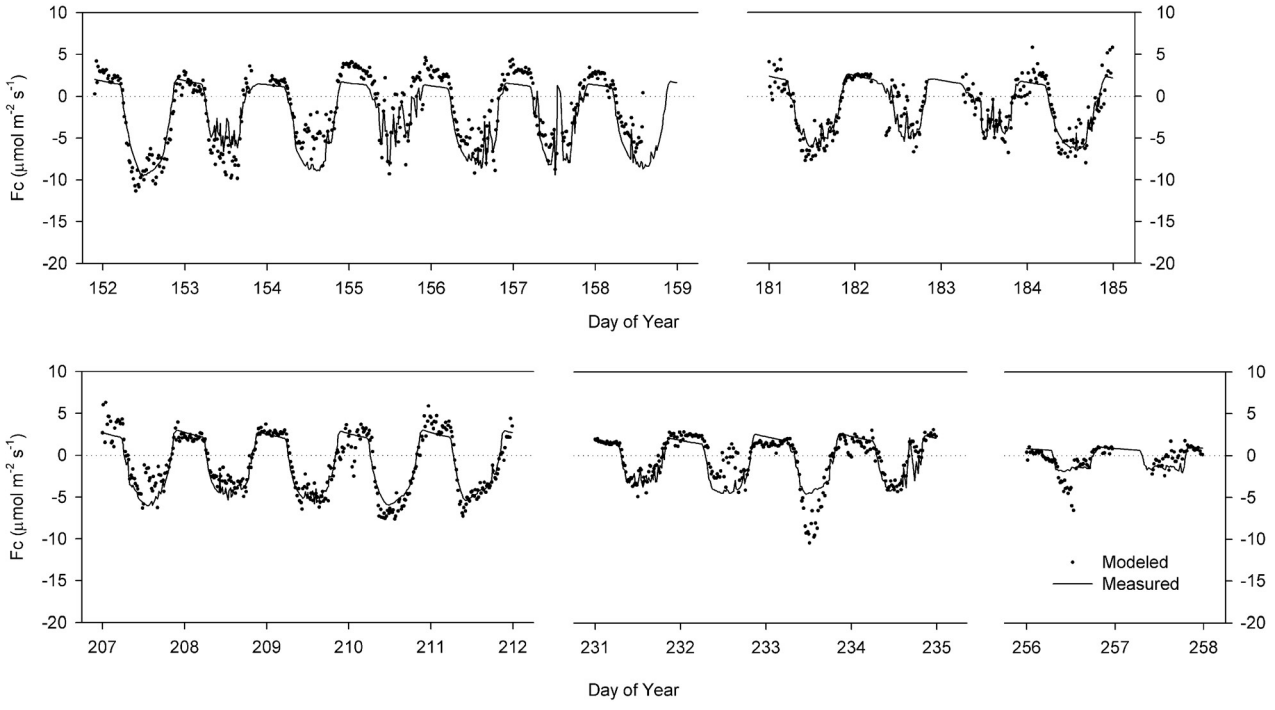

Figure 11. Daily course of CO_2 flux (Fc) for 22 days during the growing season. Dots are Fc measurements, and the solid line is predicted Fc using a combined energy balance-carbon assimilation model.

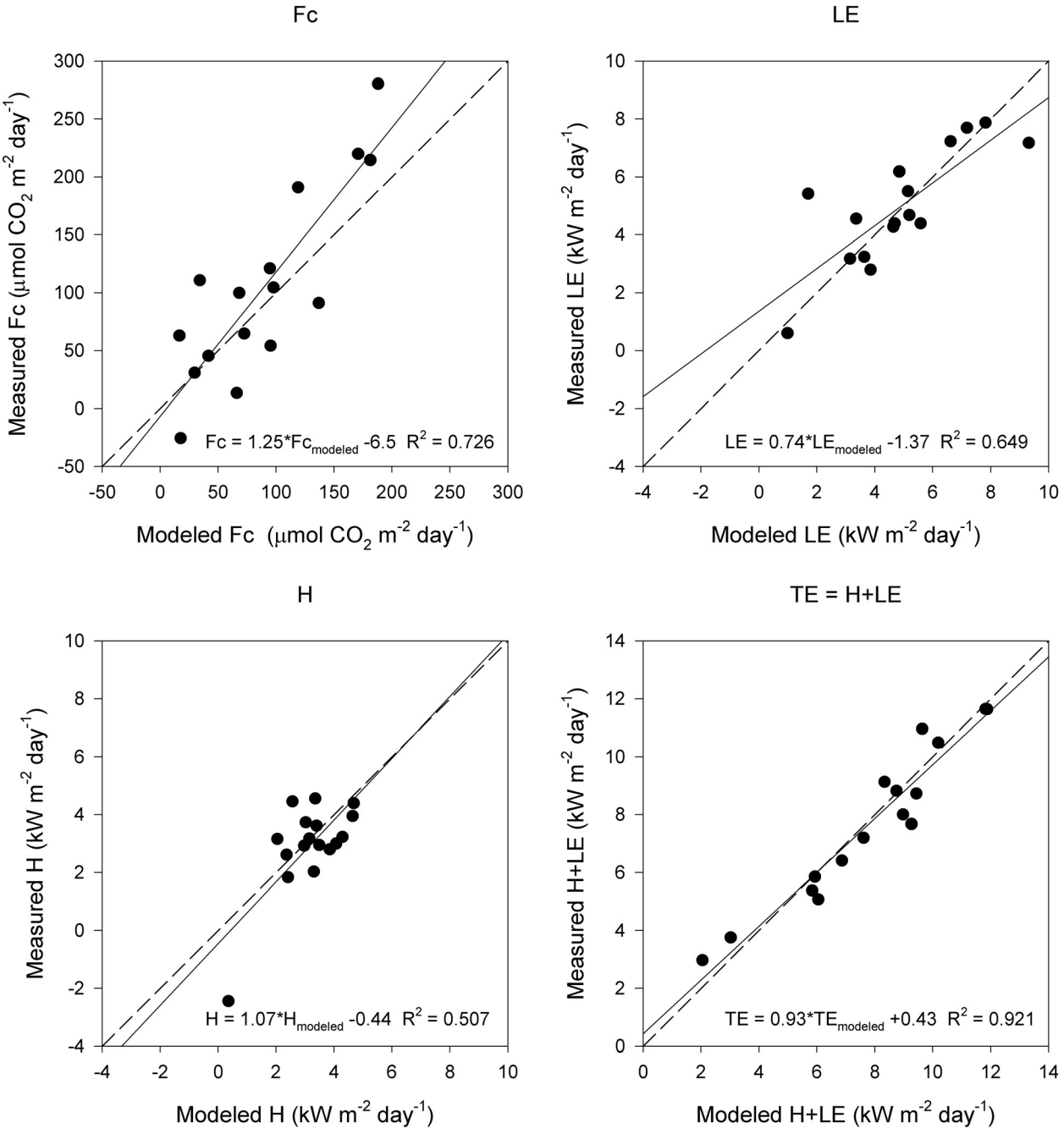

Figure 12. Scatterplots and regressions of modeled versus measured CO_2 and energy fluxes integrated during 24-hour dawn-to-dawn periods. Dashed lines are 1:1 plots; solid lines are regression plots.

the best fit parameter combination for Fc and LE to infer the pair of either Vc_{max}-**m** or LAI-**m** relationships that best fit the two fluxes. Whether Vc_{max} and LAI could have both changed during the growing season was not examined. In addition, the authors did not indicate whether their observed dramatic reductions in LAI or Vc_{max} (and smaller reduction in **m**) were consistent with the measured energy budget, especially the excluded H term.

5.1. Seasonal Patterns of Ecosystem Parameters

[60] The model inversion approach used in our study identified ecosystem parameters that predicted measured CO_2 and energy fluxes with high fidelity and little apparent bias (Table 2). These findings validated our hypothesis that this approach can be used in studies in which these ecosystem attributes have not been measured directly in the field. The ecosystem parameters identified in our study are important physical and biological descriptors of the ecosystem during the growing season. Although actual leaf growth, C and N translocation, and plant water relations represented by these leaf characteristics change continuously in response to changing internal and external conditions [*Tanaka et al.*, 2002], micrometeorological data used to estimate these parameters are also subject to mea-

Table 4. Modeled Change in LAI Parameter Compared to Leaf Area Changes Estimated by Direct Biomass and Eddy Covariance Measurement[a]

Day	Number of Days Elapsed Since Previous Measurement	EC				Field Dry Matter Samples				Model LAI; Field Dry Matter		EC		Model	
		P, μmol /day	R, μmol /day	NEE, μmol /day	Mean NEE,[b] μmol /day	NEE Days, μmol	Alive, g/m^2	Roots, g/m^2	Alive + Roots, g/m^2	Percent Above, %	SLA, m^2/g	Mean SLA,[b] m^2/g	dLAI,[c] m^2/m^2	dLAI,[d] m^2/m^2	dLAI, m^2/m^2	LAIo, m^2/m^2
155		251	60	191			194.6	143.8	338.4	0.57	0.012					2.34
183	28	184	66	118	155	4333	253.7	203.8	457.5	0.55	0.008	0.010	0.772	0.43	−0.30	2.04
209	26	151	63	88	103	2685	203.2	203.5	406.6	0.50	0.011	0.010	0.454	0.23	0.18	2.22
233	24	91	59	32	60	1446	189.4	192.4	381.8	0.50	0.013	0.012	0.305	0.15	0.13	2.35
257	24	61	27	34	33	797	56.1	323.8	379.9	0.15	0.016	0.014	0.404	0.06	0.15	2.49

[a]Carbon uptake was converted to leaf area using the following stoichiometric conversions adapted to a molar basis from *France and Thornley* [1984] after *Penning de Vries et al.* [1974]: Structural yield (SY) for leaf = 0.8653 μmol leaf μmol^{-1} substrate, inverse molecular weight of leaf (IMW) = 48.64 μmol leaf-C g^{-1} leaf, and $dLAI = \frac{\mu molCuptake}{day} \cdot \#days \cdot \frac{SY}{IMW} \cdot SLA \cdot \frac{aboveground DM}{totalDM}$, where SLA is specific leaf area (m^2 g^{-1}) and DM is measured biomass. Partitioning was assumed to correspond to the measured proportions of living above and belowground biomass.
[b]Mean values are calculated between each row and its previous row.
[c]Maximum increase in LAI if all NEE is allocated toward leaves.
[d]Increase in LAI if NEE is allocated using root:shoot partitioning.

surement errors. Some authors have addressed this measurement uncertainty by estimating ecosystem properties (i.e., light response curves, respiration rates) from flux measurements averaged across several days [*Baldocchi*, 1997]. Instead of averaging the flux measurements, we fitted single values of the parameters across a period of several days. We observed a high degree of energy balance closure for both the measurements and the model (Figure 2), which suggests that the parameter estimates are not systematically biased.

[61] The pattern of Vc_{max} in our study is consistent with typical N budgets in perennial deciduous vegetation [*Chapin*, 1980], especially range grasses [*Coppock et al.*, 1983]. In N-stressed environments, perennial plants remobilize leaf N to support root growth [*Coyne et al.*, 1995], and in our study the decline in estimated Canopy-Vc_{max} paralleled the measured increase in carbon partitioning to the roots (Table 4). Mean daily photosynthetic rates for each period (measured by EC) were closely associated with leaf and canopy Vc_{max} (Figure 6). The diurnal dynamics of photosynthesis mainly shows the ecosystem response to PAR (Figure 10), a timescale where Vc_{max} is constant. However, the seasonal results (Table 2) emphasize that this diurnal pattern is captive to a seasonal pattern in which photosynthetic response to PAR is controlled by Vc_{max}, because periods of high PAR in the later season would otherwise imply a higher photosynthetic rate.

[62] The modeled increase in LAI over the season reflects a proportional increase in absorbed incoming shortwave radiation over the season. The absorbed incoming radiation (minus ground heat flux) is balanced by total outgoing turbulent fluxes H + LE. Because H + LE in this study generally increases over the season as a proportion of incoming radiation, the model estimates that LAI increases. The modeled expansion of leaf area can also be analyzed within the context of measured photosynthesis and partitioning. A stoichiometric analysis of leaf area growth, estimated from EC measurements and field data, is presented in Table 4. Except for the initial drop in modeled leaf area, the change in leaf area based on field measurements corresponded quite closely to the modeled increase in LAI. The drop in leaf area at about day 183 and the temporary increase in aboveground dry matter may correspond to flowering and seed filling in the *Stipa* grasses. *Reekie and Bazzaz* [1987] found that reproduction in the perennial grass, *Agropyron repens* L., had little effect on total growth so the drop in LAI is probably not related to leaf senescence during flowering. However, at flowering, awns of *Stipa capillata* are exerted and can reach 10 to 20 cm in length, each having several long (5 mm) highly reflective hairs. The drop in LAI, which was solved by fitting the total outgoing energy, may be due to an increase in canopy reflectance, which effectively decreased absorption of incoming radiation and, thereby, lowered outgoing energy.

[63] Measured mean daily respiration rates changed relatively little during the growing season, although derived parameters indicated that ecosystem respiration rate increased as a proportion of photosynthetic rate, and the exponent for temperature dependence of respiration decreased. Although few ecosystem models adequately represent variation in root and soil respiration with both substrate and kinetic limitations [*Hibbard et al.*, 2004],

the observed ecosystem respiration appeared to conform to this dual-constraint paradigm. During the growing season, root mass increased both as a proportion of total mass and in absolute terms, while soil temperature generally decreased. As a result, respiration was maintained at a relatively constant rate by increasing carbohydrate supply to roots despite decreasing temperature.

5.2. Interpretation of Changes in the Ball-Berry Parameter (m)

[64] The Ball-Berry equation has been used to describe both leaf-level and canopy-level gas exchange. Although the modeling efforts cited here are chiefly concerned with CO_2 budgets, this stomatal conductance parameterization plays a major role in structuring the land surface energy balance within climate models, which demand accurate heat flux estimates. Leaf measurements showed that the Ball-Berry parameter (**m**) rarely exceeds 12 (J. Berry, personal communication, 2004), and typically is about 10 [*Baldocchi and Meyers*, 1998]. However, using a value of 10 to scale up to the canopy frequently overestimates H flux [*Leuning*, 2000]. Therefore, on the basis of tower measurements of gas exchange, modelers have varied **m** to reduce bias in the balance of energy between H and LE, often resulting in **m** values between 10 to 20 [*Zhan and Kustas*, 2001], but occasionally as low as 5.9 [*Lai et al.*, 2000]. This discrepancy can be traced to (1) methodological errors in determining **m** from canopy-level flux data, (2) stomatal behavior that is not accounted for by the Ball-Berry equation when scaled to the canopy, or (3) unmodeled features of the ecosystem that affect the energy balance.

[65] We addressed potential methodological errors in determining **m** by solving all ecosystem parameters simultaneously. Our findings agree with those of *Lai et al.* [2000] who found that models cannot accurately predict measured fluxes unless the stomatal conductance model is modified to reflect changes in the partitioning of H/LE energy. In addition, we found that these modifications in the stomatal conductance model must be integral to the solution algorithm for LAI or Vc_{max} because changing either of these canopy attributes has feedback effects on estimates of these parameters through the observed fluxes of CO_2, H_2O, and heat. Similarly, *Lai et al.* [2000] found that incorporating a correction factor for **m** simultaneously improved LE estimates while degraded estimates of Fc, possibly because Vc_{max} and the correction factor were not solved iteratively.

[66] Our study showed that there is variation in surface conductance that is not addressed in the Ball-Berry equation that is reflected in observed changes in β and λ, which are not accounted for if **m** is held constant. *Ball et al.* [1987] concluded that stomatal conductance could change either as a consequence of a change in assimilation rate (A) or plant endogenous factors that directly affect **m**. During model development, the slope of the Ball-Berry equation was allowed to change to account for observed changes in the Bowen ratio, to reflect unmodeled factors that affect stomatal conductance. This change in **m** is similar to applying correction factors that others have incorporated into the Ball-Berry Model to account for changes in stomatal behavior that are not mechanistically incorporated into the model. Our adjustment of **m** is not substantively different from the water index proposed by *Baldocchi* [1997], g_F proposed by *Sala and Tenhunen* [1996], or the fitted w_r slope correction factor proposed by *Lai et al.* [2000], except that our adjustment is solved simultaneously with LAI, Vc_{max} and β_A.

[67] The fact that canopy-inferred **m** departs from its typical leaf level value of 10, even when changes in other major canopy parameters are accounted for, is an important finding in our research. The Ball-Berry equation was derived from CO_2 and H_2O flux measurements at the leaf level, and predicts whole-leaf gas conductance per leaf area, using a single-sided treatment of leaf energy balance, which is used in the calculation of leaf temperature and leaf saturation vapor pressure. However, the model is typically applied to predict canopy-level conductance, often using two-sided treatment of leaf energy balance. In a conventional resistance framework, a two-sided leaf energy balance model doubles the conductance for H, as well as doubles the incoming and outgoing longwave radiation. Assumptions in the calculation of the conductance of longwave radiation can have a dramatic effect on the calculation of leaf temperature, thereby impacting estimated H. We conclude that the wide variety of values in use for the Ball Berry constant reflect differences among researchers in energy balance calculations used to estimate leaf temperature. In light of the widespread use of this stomatal conductance model, a synthesis of canopy energy balance models and measurements would be a valuable step in clarifying the canopy-level **m**.

6. Conclusions

[68] The goal of our study was to find a way to obtain estimates of several key ecosystem parameters from flux measurements using a widely used modeling paradigm. There are many benefits to accurately estimating these parameters from flux data. First, suspicious flux data can be highlighted in light of first principles and well-defined physical processes to determine if suspect measurements are consistent with adjacent data. Second, millions of aggregated flux data can be reduced into a small number of parameters that determine 80–95% of the carbon and energy fluxes of an ecosystem. Third, flux measurements taken at different times and locations can be compared because the ecosystem parameters are not dependent on the particular ambient environmental conditions at the time of flux measurement.

[69] Our results showed that leaf area, maximum carboxylation velocity, ecosystem respiration, and stomatal sensitivity can be solved so that the carbon and energy fluxes can be modeled with considerable fidelity. These ecosystem parameters were shown to be consistent with independent measurements of the ecosystem's seasonal dynamics. They also were closely linked to mean daily CO_2 fluxes, but are not dependent on the environmental drivers during the measurement period. The inverse estimation of these ecosystem parameters holds considerable potential for comparing ecosystems and predicting the consequences of climate change on carbon and energy exchange.

[70] The apparent discrepancy between the Ball-Berry parameter evaluated at the leaf scale and imputed from canopy-scale measurements is unclear. A combined leaf-upscaling and model inversion approach using true measurements of LAI, Vc_{max}, **m** and Ci (approximated by

δ13C) at several canopy depths should resolve this discrepancy and highlight model treatment of critical environmental drivers (such as longwave radiation and soil water content) that are responsible for this discrepancy.

[71] **Acknowledgments.** This publication was made possible through support provided by U.S. universities, host country institutions and the Office of Agriculture and Food Security, Global Bureau, U.S. Agency for International Development, under grant PCE-G-98-00036-00. The opinions expressed herein are those of the author(s) and do not necessarily reflect the views of USAID.

References

Amthor, J. S. (2000), The McCree-de Wit-Penning de Vries-Thornley respiration paradigms: 30 years later, *Ann. Bot.*, *86*, 1–20.

Baldocchi, D. (1994), An analytical solution for coupled leaf photosynthesis and stomatal conductance models, *Tree Physiol.*, *14*, 1069–1079.

Baldocchi, D. (1997), Measuring and modelling carbon dioxide and water vapour exchange over a temperate broad-leaved forest during the 1995 summer drought, *Plant Cell Environ.*, *20*, 1108–1122.

Baldocchi, D., and T. Meyers (1998), On using eco-physiological, micrometeorological and biogeochemical theory to evaluate carbon dioxide, water vapor and trace gas fluxes over vegetation: A perspective, *Agric. For. Meteorol.*, *90*, 1–25.

Baldocchi, D., F. M. Kelliher, T. A. Black, and P. Jarvis (2000), Climate and vegetation controls on boreal zone energy exchange, *Global Change Biol.*, *6*, 69–83.

Baldocchi, D., et al. (2001), FLUXNET: A new tool to study the temporal and spatial variability of ecosystem-scale carbon dioxide, water vapor, and energy flux densities, *Bull. Am. Meteorol. Soc.*, *82*, 2415–2434.

Ball, J. T., I. E. Woodrow, and J. A. Berry (1987), A model predicting stomatal conductance and its contribution to the control of photosynthesis under different environmental conditions, in *Progress in Photosynthesis Research*, vol. IV, *Proceedings of the VII International Congress on Photosynthesis*, edited by I. Biggins, pp. 221–224, Springer, New York.

Beerling, D. J., and W. P. Quick (1995), A new technique for estimating rates of carboxylation and electron-transport in leaves of C-3 plants for use in dynamic global vegetation models, *Global Change Biol.*, *1*, 289–294.

Chapin, F. S. (1980), The mineral-nutrition of wild plants, *Annu. Rev. Ecol. Syst.*, *11*, 233–260.

Chapin, F. S., and R. W. Ruess (2001), Carbon cycle—The roots of the matter, *Nature*, *411*, 749–752.

Chapin, F. S., et al. (2000), Arctic and boreal ecosystems of western North America as components of the climate system, *Global Change Biol.*, *6*, 211–223.

Claussen, M., V. Brovkin, and A. Ganopolski (2001), Biogeophysical versus biogeochemical feedbacks of large-scale land cover change, *Geophys. Res. Lett.*, *28*, 1011–1014.

Collatz, G. J., J. T. Ball, C. Grivet, and J. A. Berry (1991), Physiological and environmental-regulation of stomatal conductance, photosynthesis and transpiration—A model that includes a laminar boundary-layer, *Agric. For. Meteorol.*, *54*, 107–136.

Coppock, D. L., J. K. Detling, J. E. Ellis, and M. I. Dyer (1983), Plant-herbivore interactions in a North American mixed-grass prairie.1. Effects of black-tailed prairie dogs on intraseasonal above-ground plant biomass and nutrient dynamics and plant-species diversity, *Oecologia*, *56*, 1–9.

Coyne, P. I., M. J. Trlica, and C. E. Owensby (1995), Carbon and nitrogen dynamics in range plants, in *Wildland Plants: Physiological Ecology and Developmental Morphology*, edited by D. J. Bedunah and R. E. Sosebee, pp. 59–167, Soc. for Range Manage., Denver, Colo.

Craine, J. M., D. A. Wedin, and F. S. Chapin (1998), Predominance of ecophysiological controls on soil CO_2 flux in a Minnesota grassland, *Plant Soil*, *207*, 77–86.

de Pury, D. G. G., and G. D. Farquhar (1997), Simple scaling of photosynthesis from leaves to canopies without the errors of big-leaf models, *Plant Cell Environ.*, *20*, 537–557.

Eugster, W., J. P. McFadden, and E. S. Chapin (1997), A comparative approach to regional variation in surface fluxes using mobile eddy correlation towers, *Boundary Layer Meteorol.*, *85*, 293–307.

Eugster, W., et al. (2000), Land-atmosphere energy exchange in Arctic tundra and boreal forest: Available data and feedbacks to climate, *Global Change Biol.*, *6*, 84–115.

Farquhar, G. D., S. von Caemmerer, and J. A. Berry (1980), A biochemical-model of photosynthetic CO_2 assimilation in leaves of C-3 species, *Planta*, *149*, 78–90.

France, J., and J. H. M. Thornley (1984), *Mathematical Models in Agriculture*, Butterworths, London.

Giardina, C. P., and M. G. Ryan (2000), Evidence that decomposition rates of organic carbon in mineral soil do not vary with temperature, *Nature*, *404*, 858–861.

Gifford, R. (2001), Plant respirationm, in *Net Ecosystem Exchange*, pp. 38–42, Coop. Res. Cent. for Greenhouse Account., Canberra, A. C. T., Australia.

Goudriaan, J., and H. H. van Laar (1994), *Modelling Potential Crop Growth Processes*, Springer, New York.

Harley, P. C., and D. D. Baldocchi (1995), Scaling carbon-dioxide and water-vapor exchange from leaf to canopy in a deciduous forest.1. Leaf model parametrization, *Plant Cell Environ.*, *18*, 1146–1156.

Harley, P. C., and J. Tenhunen (1991), Modeling the photosynthetic response of C_3 leaves to environmental factors, in *Modeling Photosynthesis—From Biochemistry to Canopy*, edited by K. J. Boote and R. S. Loomis, pp. 17–39, Crop Sci. Soc. of Am., Madison, Wis.

Hibbard, K. A., B. E. Law, M. G. Ryan, and E. S. Takle (2004), Issues and recent advances in soil respiration, *Eos Trans. AGU*, *85*, 220.

Kim, J., and S. B. Verma (1990), Components of surface-energy balance in a temperate grassland ecosystem, *Boundary Layer Meteorol.*, *51*, 401–417.

Lai, C. T., G. Katul, R. Oren, D. Ellsworth, and K. Schafer (2000), Modeling CO_2 and water vapor turbulent flux distributions within a forest canopy, *J. Geophys. Res.*, *105*, 26,333–26,351.

Law, B. E., et al. (2002), Environmental controls over carbon dioxide and water vapor exchange of terrestrial vegetation, *Agric. For. Meteorol.*, *113*, 97–120.

Leuning, R. (1995), A critical-appraisal of a combined stomatal-photosynthesis model for C-3 plants, *Plant Cell Environ.*, *18*, 339–355.

Leuning, R. (2000), Estimation of scalar source/sink distributions in plant canopies using Lagrangian dispersion analysis: Corrections for atmospheric stability and comparison with a multilayer canopy model, *Boundary Layer Meteorol.*, *96*, 293–314.

Lloyd, J., et al. (1995), A simple calibrated model of Amazon rain-forest productivity based on leaf biochemical-properties, *Plant Cell Environ.*, *18*, 1129–1145.

Massman, W. J. (2000), A simple method for estimating frequency response corrections for eddy covariance systems, *Agric. For. Meteorol.*, *104*, 185–198.

MathWorks Inc. (1999), *Matlab*, Prentice Hall, Upper Saddle River, N. J.

McFadden, J. P., W. Eugster, and F. S. Chapin (2003), A regional study of the controls on water vapor and CO_2 exchange in arctic tundra, *Ecology*, *84*, 2762–2776.

McGuire, A. D., et al. (2002), Environmental variation, vegetation distribution, carbon dynamics and water/energy exchange at high latitudes, *J. Veg. Sci.*, *13*, 301–314.

Mielnick, P. C., and W. A. Dugas (2000), Soil CO_2 flux in a tallgrass prairie, *Soil Biol. Biochem.*, *32*, 221–228.

Moncrieff, J. B., Y. Malhi, and R. Leuning (1996), The propagation of errors in long-term measurements of land-atmosphere fluxes of carbon and water, *Global Change Biol.*, *2*, 231–240.

Monteith, J. L. (1990), *Principles of Environmental Physics*, CRC Press, Boca Raton, Fla.

Neter, J., M. H. Kutner, M. H. Nachtsheim, and W. Wasserman (1996), *Applied Linear Statistical Models*, 4th ed., Irwin, Homewood, Ill.

Nichol, C. J., et al. (2002), Remote sensing of photosynthetic-light-use efficiency of a Siberian boreal forest, *Tellus, Ser. B*, *54*, 677–687.

Norman, J. M. (1993), Scaling processes between leaf and canopy levels, in *Scaling Physiological Processes: Leaf to Globe*, edited by J. R. Ehleringer and C. B. Field, pp. 41–76, Elsevier, New York.

Paw U, K. T. (1987), Mathematical-analysis of the operative temperature and energy budget, *J. Therm. Biol.*, *12*, 227–233.

Paw U, K. T., and W. Gao (1988), Applications of solutions to non-linear energy budget equations, *Agric. For. Meteorol.*, *43*, 121–145.

Penning de Vries, F. W. T., A. H. M. Brunsting, and H. H. Van Laar (1974), Products, requirements and efficiency of biosynthesis: A quantitative approach, *J. Theor. Biol.*, *45*, 339–377.

Raupach, M. R. (1988), Canopy transport processes, in *Flow and Transport in the Natural Environment*, edited by W. L. Steffen and O. T. Denmead, Springer, New York.

Reekie, E. G., and F. A. Bazzaz (1987), Reproductive effort in plants. 3. Effect of reproduction on vegetative activity, *Am. Nat.*, *129*, 907–919.

Reich, P. B., M. B. Walters, and D. S. Ellsworth (1997), From tropics to tundra: Global convergence in plant functioning, *Proc. Natl. Acad. Sci. U. S. A.*, *94*, 13,730–13,734.

Reich, P. B., et al. (1998), Relationships of leaf dark respiration to leaf nitrogen, specific leaf area and leaf life-span: A test across biomes and functional groups, *Oecologia*, *114*, 471–482.

Reichstein, M., et al. (2003), Modeling temporal and large-scale spatial variability of soil respiration from soil water availability, temperature and vegetation productivity indices, *Global Biogeochem. Cycles*, *17*(4), 1104, doi:10.1029/2003GB002035.

Ripley, E. A., and B. Saugier (1978), Biophysics of a natural grassland: Evaporation, *J. Appl. Ecol.*, *15*, 459–479.
Running, S. W., et al. (1999), A global terrestrial monitoring network integrating tower fluxes, flask sampling, ecosystem modeling and EOS satellite data, *Remote Sens. Environ.*, *70*, 108–127.
Sala, A., and J. D. Tenhunen (1996), Simulations of canopy net photosynthesis and transpiration in Quercus ilex L under the influence of seasonal drought, *Agric. For. Meteorol.*, *78*, 203–222.
Schulze, E. D. (1995), Flux control at the ecosystem-level, *Trends Ecol. Evol.*, *10*, 40–43.
Schulze, E. D., et al. (1994), Relationships among maximum stomatal conductance, ecosystem surface conductance, carbon assimilation rate, and plant nitrogen nutrition—A global ecology scaling exercise, *Annu. Rev. Ecol. Syst.*, *25*, 629–662.
Sellers, P. J., et al. (1992), Canopy reflectance, photosynthesis, and transpiration. 3. A reanalysis using improved leaf models and a new canopy integration scheme, *Remote Sens. Environ.*, *42*, 187–216.
Sellers, P. J., et al. (1996a), Comparison of radiative and physiological effects of doubled atmospheric CO_2 on climate, *Science*, *271*, 1402–1406.
Sellers, P. J., et al. (1996b), A revised land surface parameterization (SiB2) for atmospheric GCMs. 1. Model formulation, *J. Clim.*, *9*, 676–705.
Shumway, R. H., and D. S. Stoffer (2000), *Time Series Analysis and its Applications*, Springer, New York.
Sinclair, T. R., C. E. Murphy, and K. R. Knoerr (1976), Development and evaluation of simplified models for simulating canopy photosynthesis and transpiration, *J. Appl. Ecol.*, *13*, 813–829.
Su, H. B., K. T. Paw U, and R. H. Shaw (1996), Development of a coupled leaf and canopy model for the simulation of plant-atmosphere interaction, *J. Appl. Meteorol.*, *35*, 733–748.
Tanaka, K., Y. Kosugi, and A. Nakamura (2002), Impact of leaf physiological characteristics on seasonal variation in CO_2, latent and sensible heat exchanges over a tree plantation, *Agric. For. Meteorol.*, *114*, 103–122.
Tanner, C. B., and G. W. Thurtell (1969), Anemoclinometer measurements of Reynolds stress and heat transport in the atmospheric surface layer, *Res. Dev. Tech. Rep. ECOM66-G22-F*, U. S. Army Electron. Command, Fort Huachuca, Ariz.
Valentini, R., J. A. Gamon, and C. B. Field (1995), Ecosystem gas-exchange in a California grassland—Seasonal patterns and implications for scaling, *Ecology*, *76*, 1940–1952.
Wang, Y. P., and R. Leuning (1998), A two-leaf model for canopy conductance, photosynthesis and partitioning of available energy I: Model description and comparison with a multi-layered model, *Agric. For. Meteorol.*, *91*, 89–111.
Webb, E. K., G. I. Pearman, and R. Leuning (1980), Correction of flux measurements for density effects due to heat and water-vapor transfer, *Q. J. R. Meteorol. Soc.*, *106*, 85–100.
Wullschleger, S. D. (1993), Biochemical limitations to carbon assimilation in C(3) plants—A retrospective analysis of the a/Ci curves from 109 species, *J. Exp. Bot.*, *44*, 907–920.
Xu, L. K., and D. D. Baldocchi (2003), Seasonal trends in photosynthetic parameters and stomatal conductance of blue oak (Quercus douglasii) under prolonged summer drought and high temperature, *Tree Physiol.*, *23*, 865–877.
Zhan, X., and W. P. Kustas (2001), A coupled model of land surface CO_2 and energy fluxes using remote sensing data, *Agric. For. Meteorol.*, *107*, 131–152.

K. Akshalov, Baraev Kazakh Research Institute for Grain Farming, Akmolinskaya oblast, Shortandy, 474010 Kazakhstan.
D. A. Johnson, U.S. Department of Agriculture–Agricultural Research Service Forage and Range Research Laboratory, Utah State University, Logan, UT 84322-6300, USA.
E. A. Laca, Department of Plant Sciences, University of California, Davis, CA 95616, USA.
N. Saliendra, U.S. Department of Agriculture Forest Service, 5985 Highway K, Rhinelander, WI 54501-9128, USA.
A. Wolf, Department of Global Ecology, Carnegie Institution of Washington, 260 Panama Street, Stanford, CA 94395, USA. (adamwolf@stanford.edu)